Finite Element Modelling for 3D Concrete Printing: Framework and Examples

RYMEŠ Jiří[1,a] , JENDELE Libor[1,b] ČERVENKA Jan[1,c *]

[1]Červenka Consulting, Na Hřebenkách 2667/55, Prague, Czech Republic

[a]jiri.rymes@cervenka.cz, [b]libor.jendele@cervenka.cz, [c]jan.cervenka@cervenka.cz,

Keywords: 3D Concrete Printing (3DCP), Additive manufacturing, Non-linear analysis, Finite Element Method (FEM)

Abstract. This study describes a novel numerical approach for simulating the structural behaviour of 3D concrete printed elements. It assesses the structural integrity both during printing at an early age and in the final mature state. The presented approach adopts the finite element method with a non-linear material model for realistic material response. The hardening of the printed paste is captured by progressively adjusting the material model parameters during the step-by-step solution. The 3D printing and load capacity assessment are analysed within a single analysis, thus the deformation occurring during printing affects the predicted load-bearing capacity. Additionally, the approach utilizes interface elements to simulate potentially weaker connections between the printed layers.

The simulation framework is illustrated in two examples: a comprehensive 3D printing and load-bearing capacity analysis of a simple wall segment and a 3D concrete printing simulation of a single-story house structure.

Introduction

Additive manufacturing, also known as 3D printing, revolutionized prototyping by offering faster, cheaper, and more customizable production compared to traditional methods like hand-crafting or injection molding. With user-friendly CAD software, 3D printing has become accessible to a wide range of creators. Recently, the construction industry adopted this technology as 3D Concrete Printing (3DCP). 3DCP boasts several advantages: optimized material usage, reduced labour demands, and the ability to create ambitious architectural designs without formwork. The rapid growth of 3DCP is evident. A review by Ma et al. [1] showed a surge in scientific publications, from less than 40 before 2016 to over 400 by 2021. This trend extends to patents and projects, indicating strong interest from both academia and industry.

3DCP brings new considerations into structural assessment. Compared to cast-in-place or precast concrete manufacturing, the layer-by-layer construction inherent to 3D printing leads to material inhomogeneity. The bond between layers typically exhibits lower mechanical performance than the bulk material [2]. Additionally, fiber-reinforced mixtures have fibers limited to individual layers, creating weaker interlayer connections. Another aspect to consider is the geometrical imperfections arising from imprecise material deposition or early-stage deformations [3]. Both interlayer bond strength and early-age deformations impact the mechanical behaviour and load-bearing capacity of 3D-printed elements. The non-linear finite element method (FEM) offers valuable insights into this behaviour.

As the 3DCP technology develops, a number of studies dealing with the stability of the 3DCP elements during printing have been published, many of them utilizing numerical tools, such as in [3-6] or see review in reference [7]. Assessment of the stability of structural elements during printing is important during the construction phase; however, for adopting 3DCP in wider engineering practice, the structural performance at the hardened state needs to be ensured. In the projects where 3DCP was utilized, it was often used to construct lost formwork, which was later filled with cast-in-place concrete with a main load-bearing function [8]. If the load-bearing function was also assigned to the 3DCP elements, simplified numerical models were used as a complementary tool to estimate the

lower bound of the loading capacity but, in principle, the approval of the local authorities was based on the results of mock-up tests [8].

This study explores the specific challenges of 3DCP and proposes a simulation framework using a time-dependent material model and finite element method solver. By incorporating non-linear material models, FEM simulations can provide realistic structural responses. Studies have shown that non-linear FEM analysis can successfully replicate buckling collapse observed during 3DCP in the lab [4]. This approach has also been applied to simulate real house structures [5]. These simulations employed time-dependent material models that account for material hardening throughout the process. The hardening process can be linked to the underlying hydration process and concrete compressive strength, allowing for the deduction of other material parameters necessary for FEM analysis [5]. The presented framework, implemented in ATENA software, is first described and then two application examples are shown.

Concrete Printing Simulation by FEM

This study presents a FEM framework for simulation of 3DCP. It is shown that FEM, otherwise widely used for analyzing reinforced concrete structures, can be utilized for assessment of the structure's performance both at the early age during printing as well as in the mature age.

Non-linear Material Modeling for Realistic Simulations. Non-linear FEM has been used for designing new structures and assessing existing ones. By integrating non-linear relationships into material laws, the finite element model can provide a more realistic insight into the structural response under prescribed load conditions. Reinforced concrete exhibits non-linear material behaviour such as concrete cracking under tensile stresses, crushing under excessive compression, or yielding and even rupturing of steel reinforcement. The model developed by Červenka et al. [9], [10] and implemented in the ATENA software package [11] simulates tensile crack development using the smeared crack approach with a crack band, in which the tensile softening is controlled through the dissipated fracture energy. In compression, a plasticity approach employing the Menetrey & Willam failure criterion is adopted [12]. The non-linear material model is illustrated in Fig. 1. Furthermore, for simulation of the reinforcement mechanical behaviour, a multilinear stress-strain relationship can be inputted both for smeared and discrete reinforcement.

Finally, interface elements with the Mohr-Coulomb material model are adopted to simulate the contact between printed layers. The model supports user-defined softening after exceeding the ultimate tensile or shear strength, which allows simulating of the potential interlayer opening or slip.

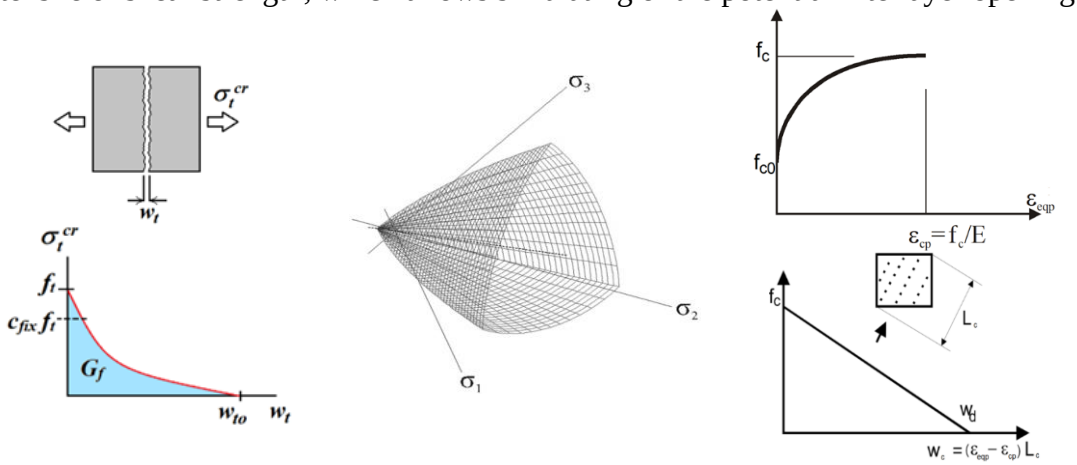

Fig. 1 The non-linear laws adopted in the material model: (left) The fracture energy softening law controlling the crack opening in tension, (middle) the Menetrey & Willam failure criterion used in compression, and (right) the hardening and softening laws for concrete crushing.

Step-by-step Simulations of 3DCP. A key aspect of the presented FEM approach in the context of 3DCP lies in its ability to simulate the actual construction process. Unlike traditional static analyses where loads are applied instantaneously, non-linear FEM employs a step-by-step approach. In this method, the loads are incrementally increased over several steps, allowing the development of non-

linear material behaviour, which typically results in redistribution of the internal forces. For 3DCP, each step in the simulation is assigned to a specific time during the printing process. Then, during the simulation run, a group of elements is activated at each step according to the printing speed and trajectory, thus the gradual construction process is simulated. The moment of an element's activation, referred to as the *element construction time*, is a key variable that is further used at each solution step for the estimation of the loads and material model parameters. This allows simulation of the material maturing and shrinkage. This step-wise approach with time-dependent load application provides a more realistic picture of the stresses and strains developing within the structure as it is being printed.

Kinetic Material Model. Accurately modelling material behaviour is essential for numerical simulations, particularly in 3DCP, where material nature evolves from a thixotropic, non-Newtonian fluid to a solid hardened paste. This study adopts the model of Červenka et al. [9], [10] and extends it with a time-dependent component to simulate the hardening paste used in 3D concrete printing. The material model thus accounts for the gradual increase in material performance. At the moment of printing, the material performance characteristics are primarily determined by the thixotropic nature of the paste. This initial phase can be further divided into two stages. First, the re-flocculation phase occurs when the interparticle bonds are re-created [13], leading to a slight increase in strength. The second mechanism is the formation of the early hydration products, referred to as the structuration phase [13], [14]. For small-scale samples that are printed in the time frame of a few hours, these two mechanisms are dominant during the printing process and the hydration after the dormant period hardens the paste already in the final shape.

In the numerical analysis, as the paste hardens, the parameters in the material model are updated for each finite element at each solution step to reflect the evolving state of the material. Each integration point within the model has unique material parameters that are updated at each solution step to reflect the ongoing hardening process based on the element construction time.

The Origin of Imperfection and the Loss of Stability. A crucial aspect of numerical simulations for the 3DCP process involves capturing the potential loss of stability of the printed element as it grows in height. This phenomenon arises from the interplay between the evolving material properties and the increasing weight of the structure during the printing process. Freshly deposited material in the lower layers of a 3D-printed element typically exhibits low yield stress, meaning it can deform significantly, even under the self-weight of the structure. As printing progresses and upper layers are added, the weight transfer by these lower layers increases. This combination of low material strength and increasing load may lead to increasing deflection in the structure. In the worst-case scenario, this deflection can progress into buckling collapse, a characteristic failure mode in additive manufacturing techniques like 3DCP.

To accurately assess the risk of stability loss, the FEM adopts the updated Lagrangian formulation. This method updates the nodal coordinates after each solution step based on the calculated deformation. This approach allows the simulation to reflect the time-dependent nature of 3DCP, where the structure continuously deforms under its self-weight as printing progresses. Furthermore, the updated Lagrangian formulation enables the inclusion of second-order effects in the overloading simulation at the mature age. This, also known as P-delta effects, accounts for the influence of the axial load acting on the element with lateral displacement. In the context of 3DCP, this becomes relevant as the deformation occurring during the printing process represents the initial imperfection during the overloading simulation.

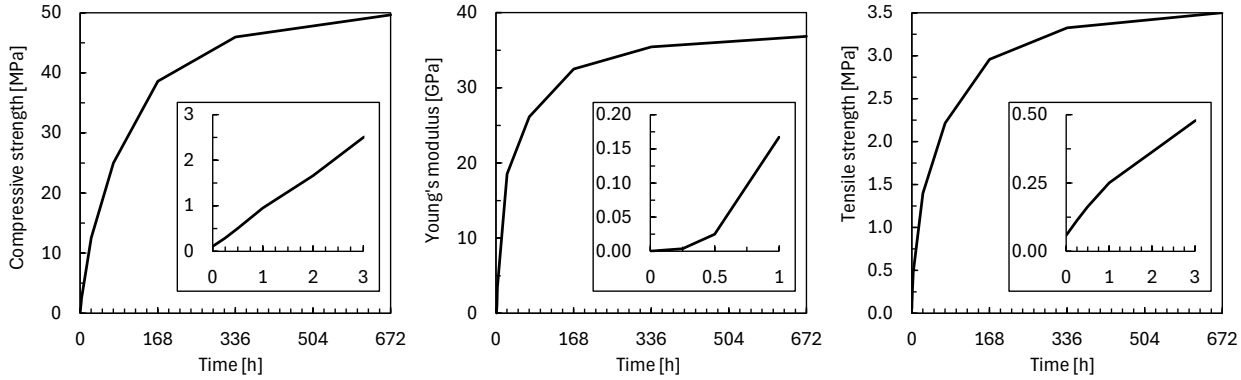

Fig. 2 Development of the material properties in the simulation of the wall segment: (left) Compressive strength, (middle) Young's modulus, and (right) Tensile strength.

Example 1: Wall Segment

A wall segment was prepared at the Klokner Institute in Prague, Czech Republic using 3DCP. The element's dimensions were (width×length×height) 300×970×800 mm and the thickness of the printed material was 20 mm. The wall segment features two internal stiffeners along the length of the element. The printing material has a compressive strength of approximately 50 MPa after 28 days. Once matured, the segment underwent compressive strength testing to assess its load-bearing capacity.

The evolutions of the key parameters of the non-linear material model that were used in the simulation are plotted in Fig. 2 throughout the simulation span. To estimate the evolution of each material parameter of the non-linear model, we used the available experimental data for compression strength at different ages and calculated the evolution of the remaining parameters using the method presented for instance in [5]. The parameters of the material model at 28 days are summarised in Table 1.

Table 1 Parameters of the material model at 28-days for the simulation of the wall segments.

Concrete	
compressive strength: f_c [MPa]	-49.64
Young's modulus: E [GPa]	36.85
tensile strength: f_t [MPa]	3.5
Poisson's ratio: v [-]	0.2
fracture energy: G_f [N/m]	147.4
plastic strain at compressive strength: ε_{cp} [-]	-0.001347
critical compressive displacement: w_d [mm]	-0.25
onset of crushing: f_{c0} [MPa]	-16.55
Horizontal (interlayer) interface	
tensile strength: f_{ti} [MPa]	0.5
cohesion: c [MPa]	0.5
friction: μ [-]	0.5
Vertical interface	
tensile strength: f_{ti} [MPa]	0.25
cohesion: c [MPa]	0.25
friction: μ [-]	0.5

A finite element model of the 3DCP wall segment was developed to replicate the experimental behaviour. The model comprised 27680 quadratic elements, each having eight nodes with three degrees of freedom. Interface elements were added between every printed layer to simulate possible interlayer slips or openings. A vertical interface element was placed in the middle of the two inner stiffeners and a loading plate was modelled at the top of the wall segment for simulation of the loading tests. The printing was simulated with a speed of 120 mm/sec and the total printing time was approximately 30 minutes, followed by the loading test simulation at 28 days. From the moment of

the element's activation until the loading test, the time-dependent initial strain with the final value of -1200 μstrain was prescribed to the model to simulate the material shrinkage. The shrinkage, however, did not significantly affect the model, mainly due to the lack of any internal or external constrains preventing the shrinkage.

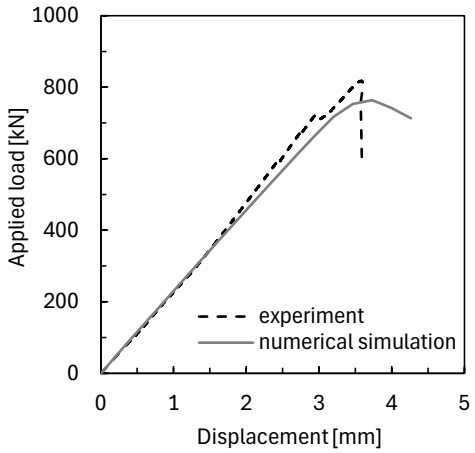

Fig. 3 The comparison of the load-displacement diagrams obtained in the experiment and from the numerical simulation.

Results. The load-displacement diagrams from the experiment and numerical simulation are compared in Fig. 3 with displacement representing the vertical displacement of the loading plate of the compression machine. The maximum load-bearing capacity of the experimental sample reaches approximately 800 kN and is well reproduced by the simulation. In Fig. 4 (left), the out-of-plane deformation in the longitudinal wall is shown. According to the analysis results, the maximum deformation after the printing reaches approximately 5.5 mm. In the subsequent steps, the maturing of the material is simulated, followed by loading of the sample to determine the maximum load-bearing capacity. At the peak load, vertical cracks develop in the middle and both corners of the longer portion of the longitudinal wall. These cracks result in out-of-plane brittle buckling and collapse of the sample under the loading as shown in Fig. 4 (middle). To illustrate the load-bearing mechanism, the normal stress in the interface elements is shown in Fig. 4 (right) at the maximum load. It can be seen that the load is transferred mainly through the internal stiffening columns and the corners of the segment while the part with the initial imperfection is less stiff and thus less loaded.

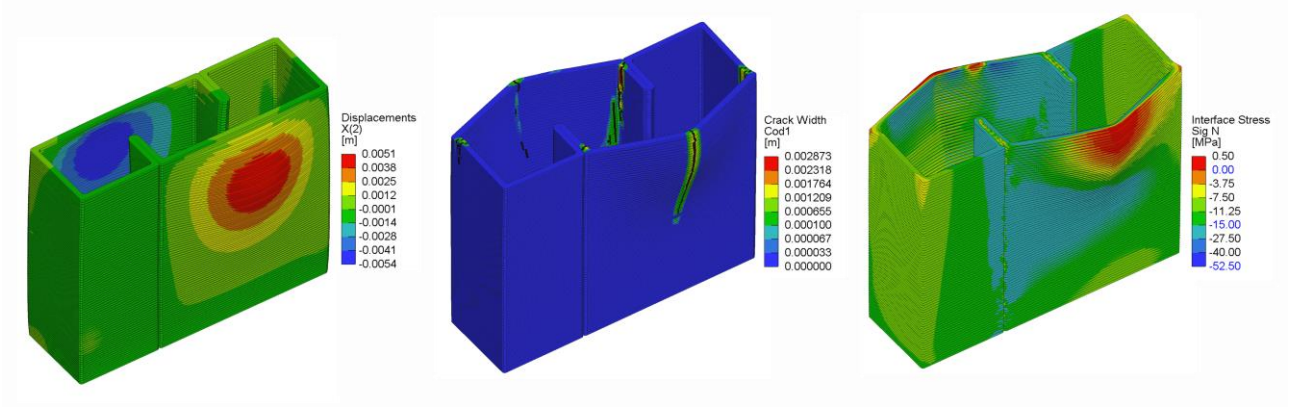

Fig. 4 Numerical simulation of the wall segment: (left) Out-of-plate displacements in the wall after printing, (middle) Crack pattern at the peak load, and (right) normal stress in the interface elements at the peak load.

The load-displacement diagram in Fig. 3 shows different behaviour in the post-peak, where the experimental data suggest more brittle bahaviour than the numerical model. This larger ductility observed in the simulation might be attributed to the slight numerical inaccuracy, more specifically to the residual forces in the interface elements during their opening on the course of the progressive collapse of the wall segment. Another factor might be the precision of the experimental data in the

post-peak related to the ability of the loading machine to quickly decrease the applied load once the peak strength of the wall was exceeded, which would overestimate the brittles of the tested segment.

Example 2: The Prvok House

The simulation framework described earlier was further adopted in the simulation of the printing process of the Prvok House, built in Prague, Czech Republic. The name "Prvok," translating to "Protozoan" in English, holds a dual meaning. It signifies the first large-scale application of 3DCP in the Czech Republic, while also referencing the house's design, which evokes the shape of these early single-celled organisms. The Prvok House features a sandwich wall structure consisting of an outer and inner surface connected by stirrup reinforcement. Each printed layer is 45 mm thick and 12 mm high. The outer wall's distinctive wavy geometry not only provides an interesting architectural aesthetic but also enhances its out-of-plane stability. In contrast, the inner wall lacks the wavy design; however, its stability is provided by sigma-shaped columns spaced approximately every half meter. A photo of the Prvok House after construction is shown in Fig. 5.

Fig. 5 The Prvok House after printing in the city center of Prague, Czech Republic (courtesy of Scoolpt s.r.o., adopted from [5]).

For the construction, a commercially available, ready-to-use fiber-reinforced concrete mix specifically formulated for 3DCP was used. The technical specifications provided by the manufacturer were used to estimate the parameters for the kinetic material model used in the simulation.

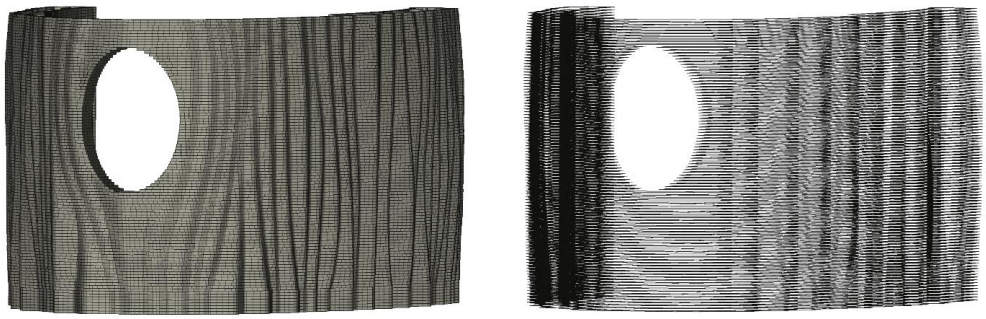

Fig. 6 Finite element model of the Prvok House: (left) Solid elements for concrete and (right) Interface elements printed between layers.

Numerical Analysis. The finite element model represents one-half of the whole structure, including the elliptical window in the front. The model is shown in Fig. 6. The simulation of the 3DCP process considers the actual building sequence as follows: First, the entire length of the wall

base was printed until the height of the front window. Second, the wall section on the left side of the window was constructed up to the top of the window opening, followed by the corresponding section on the right. Lastly, the entire section of the sandwich wall above the window was printed. The analysis assumed a total construction time of approximately 90 hours. Further details can be seen in our other study [5]. Compared to these data, the model presented here additionally employs interfaces automatically generated between the printed layers, that typically represent a weak spot in structures constructed by 3DCP.

The analysis results showing the principal compressive strain at various stages of the printing are given in Fig. 7. It can be seen that larger compressive strain is predicted on both sides of the window opening compared to the wall below and above the opening. As apparent from Fig. 7, the segments on the left and right sides of the wall were printed individually, therefore, the construction speed was approximately doubled compared to the rest of the structure. Due to higher construction speed, the material there is younger, thus having lower mechanical performance characteristics when the subsequent concrete layers are deposited. This results in higher deformation and higher strain.

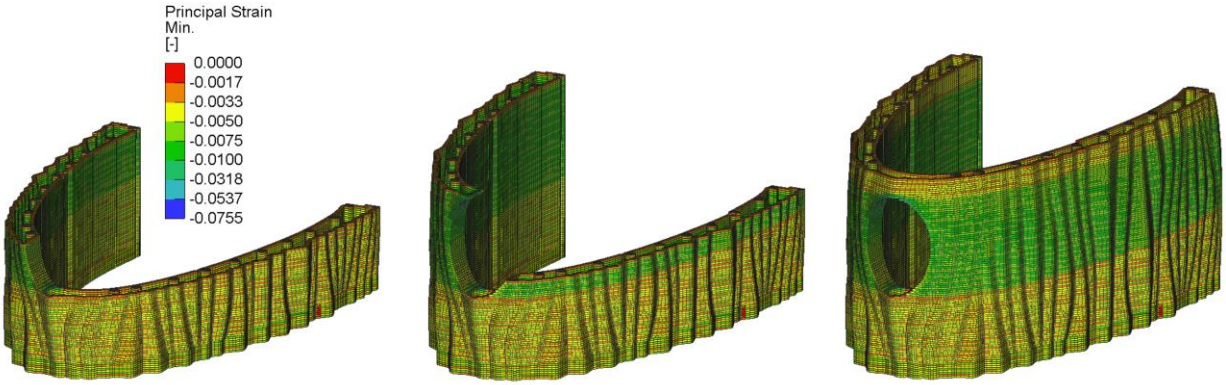

Fig. 7 Principal compressive strain at various stages of the printing of the Prvok House.

Summary

This study investigates the structural behaviour of 3DCP elements by using a comprehensive non-linear finite element method analysis. By adopting a time-dependent material model that can capture the hardening of the fresh paste, the simulation allows assessment of the structural integrity both in the fresh and mature age. The printing process is simulated by gradually activating elements along the printing path, enabling stability assessment during printing. Weaker interlayer connections are represented by interface elements within the model. Early-age deformations occurring during printing are kept in the simulation, influencing the structural response during the simulated mature-age load test. The validity of the FEM model is assessed by comparing load-displacement curves and failure modes from the analysis with experimental results. Furthermore, another simulation result is shown for a single-story house structure with a complex architectural design.

This study demonstrates the potential of non-linear FEM for comprehensive evaluations of 3DCP element structural integrity from early-age to mature stages.

Acknowledgements

This study was supported by the Czech Technology Agency and Ministry of Industry and Commerce under the program TREND and project no. FW06010422 “Simulation and design of structures from digital concrete”. The financial support is greatly acknowledged.

The experimental data for the wall segment were obtained at the Klokner Institute, Prague, Czech Republic in collaboration with the Technical University of Liberec, Czech Republic. The authors express gratitude to these institutions for providing the data for this study.

References

[1] G. Ma, R. Buswell, W.R. Leal da Silva, L. Wang, J. Xu, S.Z. Jones, Technology readiness: A global snapshot of 3D concrete printing and the frontiers for development, Cem. Concr. Res. 156 (2022) 106774.

[2] E. Keita, H. Bessaies-Bey, W. Zuo, P. Belin, N. Roussel, Weak bond strength between successive layers in extrusion-based additive manufacturing: measurement and physical origin. Cem. Concr. Res. 123 (2019), 106774.

[3] R. J. M. Wolfs, P. Bos Freek, and T. A. M. Salet, Early age mechanical behaviour of 3D printed concrete: Numerical modelling and experimental testing, Cem. Concr. Res. 106, 2018, 103-116.

[4] M. Vaitová, L. Jendele, J. Červenka, Printing of Concrete Structures Modelled by FEM, Solid State Phenom. 309 (2020), 261–266.

[5] J. Rymeš, J. Červenka, L. Jendele, Material Modelling and Simulation of 3D Concrete Printing Process, In: J. M. Chandra Kishen, A. Ramaswamy, S. Ray, R. Vidyasagar (Eds.), Proceedings of FraMCoS-11, 2023.

[6] D. An, Y. X. Zhang, and R. C. Yang, Numerical modelling of 3D concrete printing: Material models, boundary conditions and failure identification. Engineering Structures, 299 (2024), 117104.

[7] S. A. Khan, , and M. Koç, Numerical modelling and simulation for extrusion-based 3D concrete printing: The underlying physics, potential, and challenges. Results in Materials, 16 (2022), 100337.

[8] F. P. Bos, C. Menna, M. Pradena, E. Kreiger, W. L. da Silva, A.U. Rehman, D. Weger, R. J. M. Wolfs, Y. Zhang, L. Ferrara, and V. Mechtcherine, The realities of additively manufactured concrete structures in practice. Cem. Concr. Res., 156 (2022), 106746.

[9] J. Červenka, V. Červenka V, R. Eligehausen, Fracture-plastic material model for concrete, application to analysis of powder actuated anchors. In: H. Mihashi, K. Rokugo (Eds.), Proceedings FraMCoS-3, 1998, 1107–1116.

[10] J. Červenka, V. K. Papanikolaou, Three-dimensional combined fracture–plastic material model for concrete. Int. J. Plast. 24 (2008), 2192–2220.

[11] V. Červenka, L. Jendele, J. Červenka, ATENA Program Documentation: Part 1 Theory, Prague, 2023.

[12] P. Menetrey, K. J. Willam, Triaxial failure criterion for concrete and its generalization. Structural Journal, 92(3) (1995), 311-318.

[13] N. Roussel, A thixotropy model for fresh fluid concretes: Theory, validation and applications, Cem. Concr. Res. 36 (2006), 1797–1806.

[14] J. Kruger, S. Zeranka, G. van Zijl, An ab initio approach for thixotropy characterisation of (nanoparticle-infused) 3D printable concrete, Constr. Build. Mater. 224 (2019), 372–386.